



Comparison of Joint Models Used for the Propagation of Shear Waves Across Jointed Rocks

Kallol Saha^{1[0000-0003-3159-7420]}, Dr. Resmi Sebastian²

^{1,2}Department of Civil Engineering, Indian Institute of Technology, Ropar, Punjab-140001
kallol001.saha@gmail.com
resmisebastian@gmail.com

Abstract. Shear waves are generated in jointed rocks due to various sources such as earthquakes, mining, blasting etc. Strains of varying levels get developed in the rocks, due to seismic wave propagation, depending on the medium of propagation and distance between vibration source and area of interest. This paper describes the numerical simulation of a test facility that generates shear waves in rock plates. The numerical simulations have been developed with the help of three-dimensional distinct element code (3DEC). To represent the material behavior of discontinuities, two models i.e., Coulomb slip (CS) joint model and continuously yielding (CY) joint model have been used. Coulomb slip model assigns elastic stiffness, frictional, cohesive and tensile strength to joint, whereas, continuously yielding joint model simulates continuous weakening behavior due to accumulation of plastic shear displacement. The test facility consists of friction bar, incident and transmitted plates. The friction bar generates shear wave in the incident plate due to its sliding movement. The validation of these numerical simulations has been done by comparing the peak particle velocities and peak particle displacements developed at the monitoring locations of incident and transmitted plates in the laboratory and in the numerical model. Parametric studies on the shear wave propagation have been conducted by varying the joint properties, in-situ normal stress, applied load magnitude and the results are presented in this paper.

Keywords: Shear wave, particle velocity, jointed rocks, wave propagation, wave amplitudes, coulomb slip model, continuously yielding joint model.

1 Introduction

Generally, rock mass present in nature have numerous discontinuities, i.e., faults, joints, fissures etc. within it. Dynamic stability of various important underground structures built on rocks depends on quality of rock mass, and also on the nature and areal extent of the discontinuities and the vulnerability due to their presence. Several researchers ([1], [2], [3], [4]) have mentioned the requirement of stability analyses of underground structures made in rocks under dynamic loading. Among the field tests, cross-hole techniques have been found to be effective in providing reliable results for studying wave propagation across rock joints ([5], [6], [7]).

Pyrak-Nolte et al. (1990 a,b) and Myer et al. (1990) studied the effect of single joint and one joint set in rock mass under dynamic loading ([8], [9], [10]). The joint parameters have been found to have significant effects on conversion of energy during wave propagation across the joint. The joint acts as a low-cut frequency filter by allowing waves having higher frequency than a specific frequency, to pass through it. Zhao et al. (2006a) conducted laboratory tests to get insights about wave propagation across one joint set. Method of characteristics (MC) method was used by researchers [11] to compute the transmitted pulses and the results were compared with the transmitted pulses captured across the joints during laboratory tests. Wave propagation across a filled joint was also studied through a modified SHPB [12] Generally, damage of rock structures under dynamic loads are regulated based on the threshold values of peak particle acceleration, peak particle velocity and peak particle displacement. Researchers ([13], [14], [15]) identified the peak particle velocity (PPV) as the major stability criterion for engineering structures in and on rocks.

Continuum, discontinuum and coupled methods are adopted in rock mechanics for conducting the numerical studies. The continuum methods like Finite Element Method (FEM) ([16]), the Finite Difference Method (FDM) ([17]) etc. assume rock mass as continuum. While dealing with large-scale fracture or complete detachment, discontinuum methods like Discontinuous Deformation Analysis (DDA) ([18]), Distinct Element Method (DEM) ([19]) are preferred. To overcome the limitations of continuum and

discontinuum methods, coupled methods have been developed in recent years. 3-Dimensional distinct element code (3DEC) [20] developed by the Itasca consulting group, Inc., comes under the DEM category. 3DEC is based on a dynamic time domain algorithm, which solves the equations of motion of a blocky system by an explicit FDM technique. DEM technique, like 3DEC represents rock mass as a group of discrete blocks. Joints are represented as interfaces between these discrete blocks ([21], [22]).

This paper presents numerical simulation of the shear wave propagation across jointed granite rocks. Experiments were conducted on SSP setup having friction bar and supporting block made up of mild steel, incident and transmitted plates made up of granite rocks. The experiments were numerically simulated by commercial software 3DEC. Two joint models available i.e., Coulomb slip (CS) joint model and Continuously Yielding (CY) joint model were used for analysis. Energy coefficients and transmission amplitude coefficient have been determined and their results have been compared with the experimental results.

2 Laboratory experiments using Split Shear Plates

The motivation of this work originated from the Split-Hopkinson pressure bar (SHPB) or Kolsky bar, an apparatus for testing the dynamic stress–strain response of solid materials such as metals, rocks, concrete etc. at high strain rates. Traditionally, SHPB has been used for the study of compression wave propagation. Liu et al. [20] developed Split shear plate (SSP) facility using the direct shear model [21] and SHPB theory for studying the shear wave propagation.

Split Shear Plate (SSP) set up used for conducting this study consists of a friction bar, an incident plate, a transmitted plate and a supporting block, as shown in Fig. 1. and 2. Granite plates were used as the incident and transmitted plates. Tables 1 and 2 shows details of dimensions and material properties. A dynamic impact mechanism provides an impact force to the friction bar in Y-direction, which creates a compression wave in the friction bar. The friction bar was kept on two rollers to help it in sliding in the y-direction. Both the rock plates (incident and transmitted plates) were supported by four supporting bars beneath them. The friction between these supporting bars and rock plates were kept negligible by making the contact surfaces as smooth as possible. The incident and transmitted plates were tightly pressed by friction bar and supporting block. The friction bar contained grooves on the inner side, to help it generate sufficient friction at the interface of the friction bar and the incident plate. This in turn generated shear wave propagating from the start of incident plate in the X direction, while compression wave traveled in friction bar in Y direction. Four piezo-electric accelerometers were attached on the incident and transmitted plates at A, B, C and D locations (as shown in Fig. 1). Point A denotes the location on the top surface of friction bar, where compression wave propagated. Acceleration-Time (a-t) history recorded at the point A is shown in Fig. 3. Points B and C denote the locations 30 mm and 640 mm distance from the start of the incident plate. Point D denotes the location at 30 mm distance from the right end of incident plate. All the accelerometer records were collected by a data acquisition (DAQ) system, which in turn was connected to a laptop.

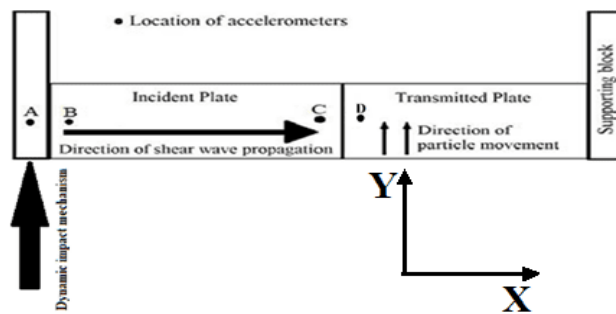


Fig. 1. Schematic diagram of Split shear plates.

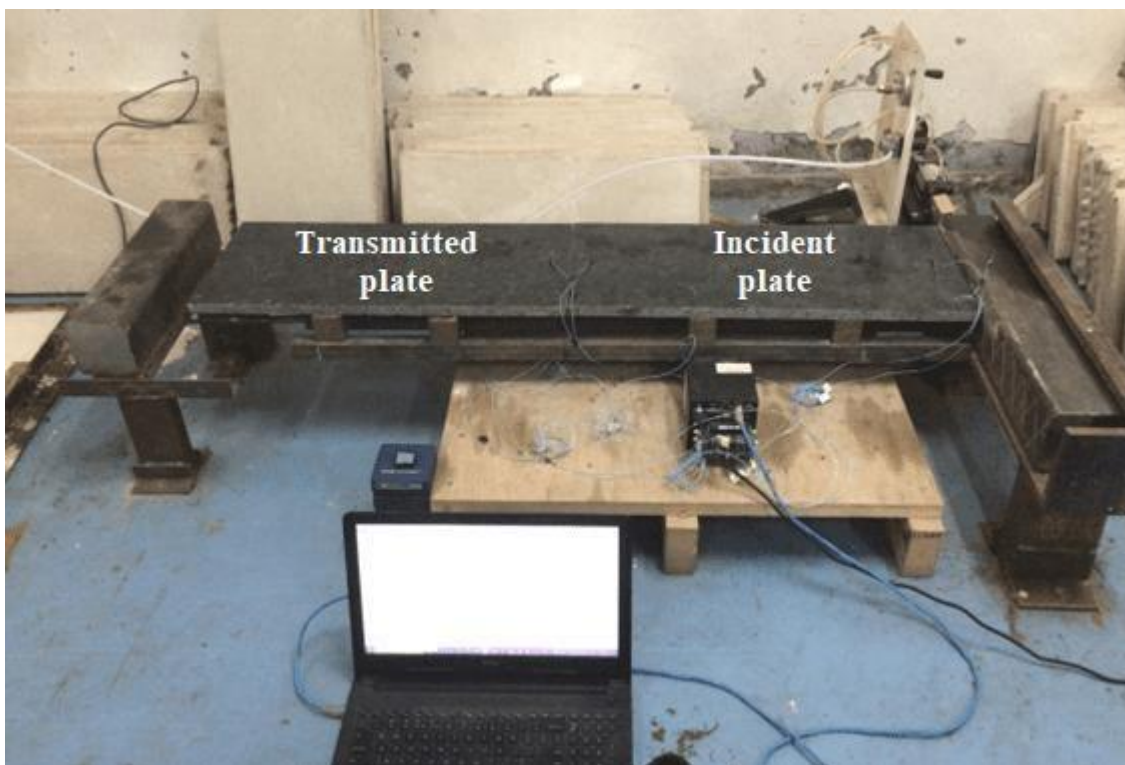


Fig. 2. Entire SSP test setup having incident plate, transmitted plates, friction bar and dynamic triggering system.

Table 1. Properties and dimensions of blocks used to describe the SSP setup

Sl. No.	SSP Apparatus components	Dimensions (mm*mm*mm)	Material	Density (kg/m ³)	Shear Modulus (GPa)	Bulk Modulus (GPa)
1	Friction bar	(100*600*100)	Mild Steel	7850	80	140
2	Incident and transmitted plate	(670*300*30) (630*300*30)	Granite	2700	6	10
3	Supporting bar (beneath rock plates)	(50*300*50)	Mild Steel	7850	80	140
4	Supporting block	(100*600*100)	Mild Steel	7850	80	140

Table 2. Engineering properties of Granite rock samples used for the study

Properties	Values
Density	2700 kg/m ³
P wave velocity	4500 to 5000 m/s
S wave velocity	2500 to 3000 m/s
Poisson's ratio	0.25
Shear modulus	17 GPa
Young's modulus	42.5 GPa

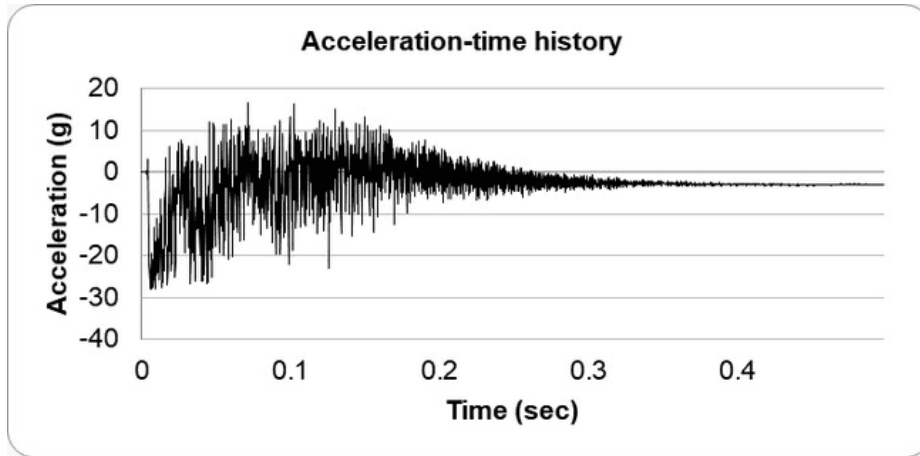


Fig. 3. Acceleration-time history of dynamic load measured in the friction bar

For the present study, the effect of joint on shear wave propagation was obtained by comparing the energy coefficients and transmission amplitude coefficients obtained for these granite rocks. The acceleration-time (a-t) history obtained from the accelerometers was integrated to determine the particle velocity-time (v-t) and particle displacement-time (d-t) histories.

From the particle velocities obtained at the rock plates (using both experimental and numerical simulation), energy flux associated with the propagating waves was calculated, using the equation obtained from [22,23].

$$E_{I/R/T} = \rho V_{Shear} \sum_t^{T_p+t} V_{Particle}^2 \quad (1)$$

where, $E_{I/R/T}$ denote the energy flux per unit area per cycle of oscillation for the incident, reflected and transmitted wave respectively.

V_{Shear} denotes velocity of propagating shear wave.

$V_{particle}$ denotes particle velocity (in perpendicular to the direction of shear wave propagation).

T_p denotes time period of the incident, reflected and transmitted wave.

From [22], energy coefficient of transmission can be obtained as

$$T = \left(\frac{E_T}{E_I} \right)^{\frac{1}{2}} \left(\frac{\gamma_1}{\gamma_2} \right)^{\frac{1}{2}} \quad (2)$$

$$\text{where, } \gamma = (G\rho)^{\frac{1}{2}} \quad (3)$$

γ_1 and γ_2 indicate seismic impedance of medium 1 (incident plate) and medium 2 (transmitted plate) respectively. As same material is being used in both the rock plates, ratio of γ_1 and γ_2 are kept as 1.0.

The coefficient of reflection, R, was defined as,

$$R = \left(\frac{\text{Energy remaining at location C for } 90^\circ \text{ jointed sample}}{\text{Incident Energy at location B for } 90^\circ \text{ jointed sample}} - \frac{\text{Energy remaining at location C for intact sample}}{\text{Incident Energy at location B for intact sample}} \right)^{\frac{1}{2}} \left(\frac{\gamma_1}{\gamma_2} \right)^{\frac{1}{2}} \quad (4)$$

Coefficient of absorption can be obtained as:

$$A = \left(\frac{E_A}{E_I} \right)^{\frac{1}{2}} = [1 - R^2 - \left(\frac{\gamma_1}{\gamma_2} \right) T^2]^{\frac{1}{2}} \quad (5)$$

where,

E_I , E_R and E_T denote energy flux associated with the incident, reflected and transmitted waves.

Shear modulus have been obtained using the shear wave velocities in the plates. The shear wave velocity was determined using first arrival of waves in a-t history obtained with the accelerometer located on both ends of each plate.

V_{Shear} was obtained from the ratio of distance between two accelerometers located on incident/transmitted plate to the time required for the shear wave to travel between two accelerometers on respective plates.

$$G_{\text{Max.}} = \rho V_{\text{Shear}}^2 \quad (6)$$

The transmission amplitude coefficients across the joints with respect to displacement and velocity i.e., T_v and T_d were determined by dividing the displacement and velocity amplitudes obtained after the joint (in transmitted plate) by the particle displacement and velocity amplitudes obtained before the joint (in incident plate) respectively.

3 Numerical simulation using 3-Dimensional Distinct Element Code (3DEC)

Numerical modeling is an economical approach to study the wave propagation across rock joints. Representing rock joints is a key challenge in numerical modelling of wave propagation through rocks. Traditionally, continuum methods have been used very frequently for such analysis. In continuum method, materials are assumed to be homogeneous, isotropic, continuous and independent of any particular coordinate system. These assumptions make continuum methods incompatible for dealing with complete detachment of elements from one another.

To overcome these limitations, a discontinuum method like DEM is chosen for representing the jointed rock mass. The joints are treated as boundary conditions between blocks. Finite displacements along the joints and rotations of discrete blocks are allowed. DEM also recognizes new contacts automatically as the calculation progresses. Among the four methods of DEM i.e., distinct element programs, modal methods, discontinuous deformation analysis and momentum-exchange methods, the first method has been chosen for simulating the jointed rock mass in this paper. 3DEC by Itasca Consulting Group Inc. comes under category of distinct element programs. 3DEC program assume the joints to be deformable and blocks to be rigid or deformable. 3DEC uses explicit time-marching methods to directly solve the equations of motion. To obtain good accuracy, the increments should be small enough, therefore this method is quite time consuming.

Numerical simulation in 3DEC requires following steps, (i) model generation, (ii) setting up boundary and initial conditions, (iii) loading and sequential modelling, (iv) choice of joint constitutive models and material properties and (v) result interpretation. The experimental SSP setup was modeled as per exact dimensions in 3DEC. Joints were provided at three required locations. Material properties of mild steel and granite rocks were assigned to respective blocks. Deng et al. (2012) ([24]) and Kuhlemeyer and Lysmer (1973) [25] suggested the mesh size of the finite difference elements should be smaller than $1/32^{\text{nd}}$ and $1/8^{\text{th}}$ of the wavelength of propagating wave respectively. Taking this into consideration, the mesh size or average edge length of tetrahedral element was selected to be 33 mm. Numerical simulation model of SSP set up is given in Fig. 6. Then, joint 1 and joint 2 are made non-reflecting viscous joints, to make sure no waves get reflected back into the model from those boundaries. Particle velocity in X and Z direction were made zero in both ends of the granite rocks. Only particle velocity at the Y direction was allowed. Impulse loading was provided in the model in form of velocity, in the +Y direction at the middle of the friction bar. The elastic-isotropic block constitutive model has been used in the presented numerical analysis, as this model can represent homogeneous, isotropic, continuous materials exhibiting linear stress-strain behaviour. This model requires the three material parameters of density (ρ), bulk modulus (K) and shear modulus (G) of the material.

The effect of two joint models on wave transmission across rock joints used in 3DEC has been considered. Joint material constitutive models define the normal and shear interaction between the blocks at their contact points. By default, CS joint constitutive model (joint area contact) is used in 3DEC, whenever closely packed blocks are present having area contacts, which works on the principle of Coulomb friction law. Parameters like joint stiffness (normal and shear) (k_n and k_s), friction angle (θ) and dilation, cohesion (C) and tensile strength are required as inputs for this joint model.

The CS joint model, shear and normal stresses on the joint get developed in the elastic model, when the stress reaches its peak strength (S_f^{peak}).

$$S_f^{\text{peak}} = C + \sigma_n \tan \theta \quad 6.(a)$$

where c , ϕ and σ_n denote cohesion, friction angle and normal stress respectively.

After the peak shear strength is achieved, the shear strength drops to the residual shear strength (S_f^{res}).

$$S_f^{res} = C_{res} + \sigma_n \tan \phi_{res} \quad 6.(b)$$

C_{res} and ϕ_{res} denote residual cohesion and residual friction angle respectively. C_{res} and ϕ_{res} are taken as zero while using CS joint model.

Shear stress-shear displacement relation has been shown in Fig. 4.

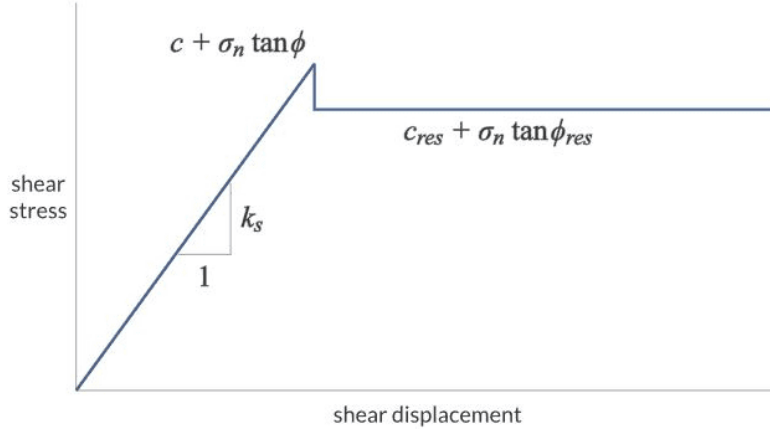


Fig 4. Shear stress-shear displacement behaviour of Mohr-Coulomb joint model. (3DEC manual, Itasca)

A comprehensive displacement-weakening model; CY joint model simulate the progressive damage mechanism of joint under shear by incorporating progressive loss in cohesive and tensile strength, as the wave propagates through the joints. Cundall et al. (1984, 1990) ([26] and [27]) proposed CY joint model to represent rock joints showing progressive damage due to accumulated plastic shear displacement.

The response to normal loading increases linearly with normal displacement

$$\Delta \sigma_n = k_n \Delta u_n \quad 7. (a)$$

where, normal stiffness, $\Delta k_n = a_n \sigma_n^{e_n}$ 7. (b)

a_n and e_n are model parameters. Generally, is assumed to be zero.

During shearing, the model shows an irreversible, nonlinear behaviour from the beginning of shearing.

Fig. 5 shows a typical stress-displacement curve for monotonic loading under constant normal stress.

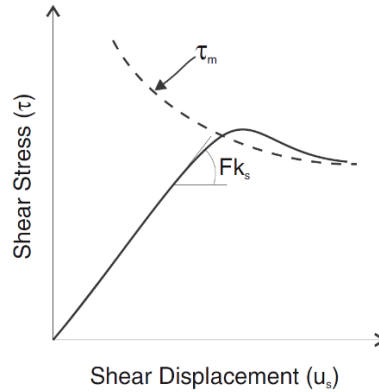


Fig. 5. CYJ model: shear stress-displacement curve (solid line curve) and bounding shear strength (dotted line curve).

The shear stress increment is calculated as

$$\Delta r = F k_s \Delta u_s \quad 7. (c)$$

where, shear stiffness, $\Delta k_s = a_s \sigma_n^{e_s}$ 7. (d)

where a_s and e_s are model parameters.

And F is tangent modulus in Eq. 7. (c). F depends on the distance from the actual stress (solid line curve) to the bounding strength (dotted line curve), r_m , shown in Fig. 5.

$$F = \frac{(1-r)}{1-r} \frac{r_m}{1-r} \quad 7. (e)$$

The r factor is initially zero. r is kept limited to 0.75 to avoid numerical noise when the shear stress is approximately equal to the bounding strength, r_m .

$$r_m = \sigma_n \tan \phi_m \operatorname{sgn}(\Delta u_s) \quad 7. (f)$$

Where, ϕ_m is the friction angle that would apply if the joint would dilate at the maximum dilation angle. As the damage keeps on accumulating, ϕ_m starts reducing according to following equation,

$$\Delta \phi_m = -\frac{1}{R_n} (\phi_m - \phi) \Delta u_s^{plastic} \quad 7. (g)$$

where the plastic displacement increment is defined as

$$\Delta u_s^{plastic} = (1-F) |\Delta u_s| \quad 7. (h)$$

Where, ϕ is the basic friction angle of rock surfaces.

ϕ_m is the effective friction angle, if no asperities were sheared off.

R is a material parameter expressing roughness of joint. It has dimension of length.

$\phi_m R$ controls the rate at which ϕ_m decreases with plastic shear displacement. A small R value causes ϕ_m to decrease faster; a large value of R leads to a slower reduction of ϕ_m and therefore to a larger peak stress. The peak is reached when $r_m = r$.

Joint properties used to describe the SSP setup in numerical model (both CS and CY joint model) are provided in Table 3 (a) and (b).

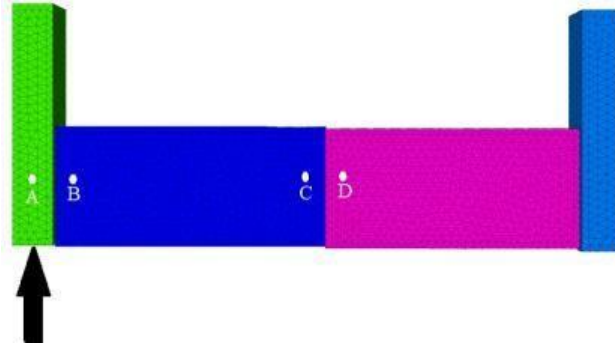


Fig. 6. Numerical simulation model of SSP set up.

Table 3. (a). Properties of joints (joint 1 and joint 2) used to describe the SSP setup in numerical model (both CS and CY joint model)

Joint	Location	Joint normal stiffness (MPa/m)	Joint shear stiffness (MPa/m)	Joint friction (degrees)
Joint 1	Joint between friction bar and incident plate	200	100	45
Joint 2	Joint between transmitted plate and supporting block	200	100	45

4 Results and discussions

The laboratory tests were conducted on jointed granite rock plates to obtain peak particle velocity and peak particle displacements at four given locations. Energy coefficients (T, R, A) were obtained from laboratory test and the joint parameters like joint stiffness (shear and normal), joint friction angle, joint cohesion, joint tensile strength have been varied to find the validated value. Table 3. (b) shows values used for the validation of the numerical model (for both CS and CY joint models). Table 4. (a) shows energy coefficients (T, R, A) obtained from laboratory experiments. Table 4. (b) shows the comparison of transmission amplitude coefficient with respect to particle velocity and particle displacement (T_v and T_d)

with laboratory and numerical simulation. Table 5 shows the comparison of T_v and T_d values obtained from parametric studies.

Table 3. (b). Validated joint parameters of joint 3 for both CS and CY joint model

Joint Parameter	CS joint model	CY joint model
JkN (GPa)	25	20
JkS (GPa)	09	04
jCoh (MPa)	2.5	2.5
jTensile (GPa)	1	1
jFric	25	25
Insitu stress (MPa)	0.5	0.5
Roughness parameter (r)	NA	0.1 mm

Table 4. (a) Energy coefficients (T, R, A) obtained from laboratory experiment

Energy coefficients	Laboratory Experiment
Transmission (T)	0.32
Reflection (R)	0.45
Absorption (A)	0.78

Table 4. (b) Comparison of transmission amplitude coefficient with respect to particle velocity and particle displacement (T_v and T_d) with laboratory and numerical simulation

Transmission Amplitude	Laboratory Experiment	Numerical Simulation	
		CY joint model	CS joint model
With respect to particle velocity (T_v)	0.82	0.85	0.79
With respect to particle displacement (T_d)	0.78	0.67	0.56

4.1 Parametric study using numerical simulations

Parametric studies were conducted to assess the significance of various joint properties i.e., joint stiffness (normal and shear), joint friction, joint cohesion, normal stress and velocity coefficient in obtaining the particle velocities and displacements from numerical simulations. Velocity coefficient is defined as the ratio of particle velocity provided in numerical modelling and actual particle velocity recorded during experiment. Transmission amplitude coefficient was obtained using particle velocity and displacements obtained from laboratory test and numerical simulations.

4.1.1 Joint shear stiffness (jks)

The joint shear stiffness value for both the CS and CY joint models was found to be 3.5 GPa/m for the validated numerical model. It was varied from 2 GPa/m to 5 GPa/m during numerical simulation keeping values of all other parameters constant. T_v and T_d were found to be increasing with an increase in jks. T_v and T_d values for CS joint model were found to be smaller than the CY joint model.

For the CY model, the particle velocity and displacement measured at location B and C (at the incident and transmitted plates at 60mm distance) vary less than that of CS model as shown in Fig. 7 (b). For CS joint model, there was a significant difference between peak particle velocity and displacement before and after the joint. This phenomenon was quite expected, because the CY joint model shows progressive damage to the material, as the wave continues to propagate from the incident plate.

In Fig. 7 (a) and 7 (b), each colored line show particle velocity before and after the joint. The curved colored line at the top and bottom (of both the figures) shows particle velocity before and after the joint respectively.

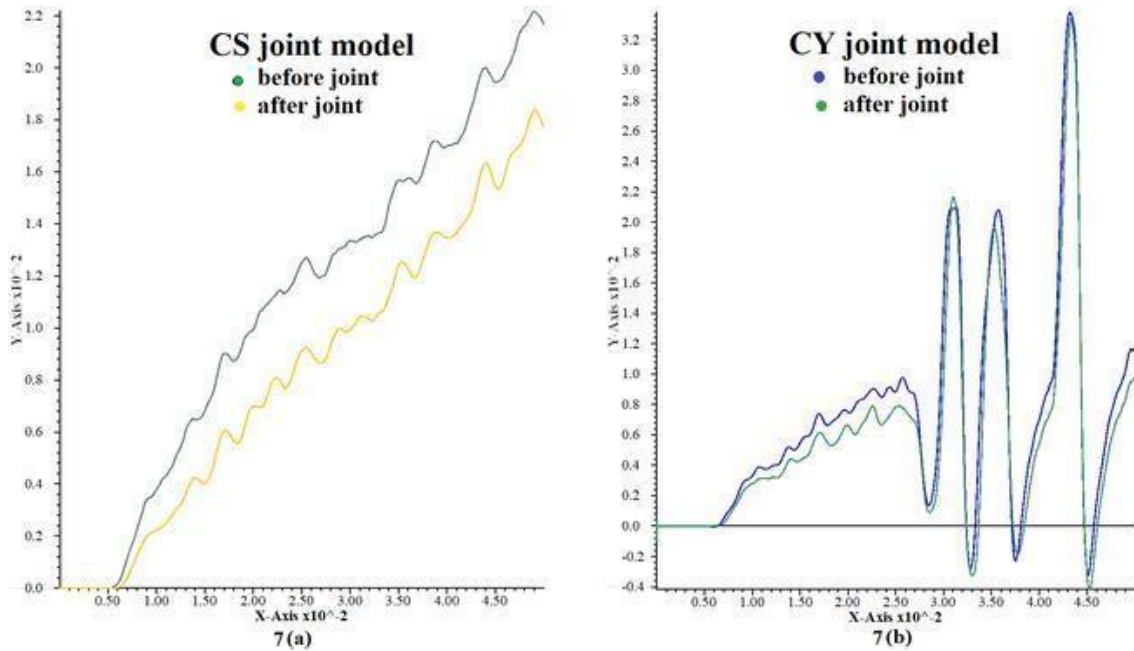


Fig. 7 (a), (b) Particle velocity for CS and CY joint model for before and after the joint location.

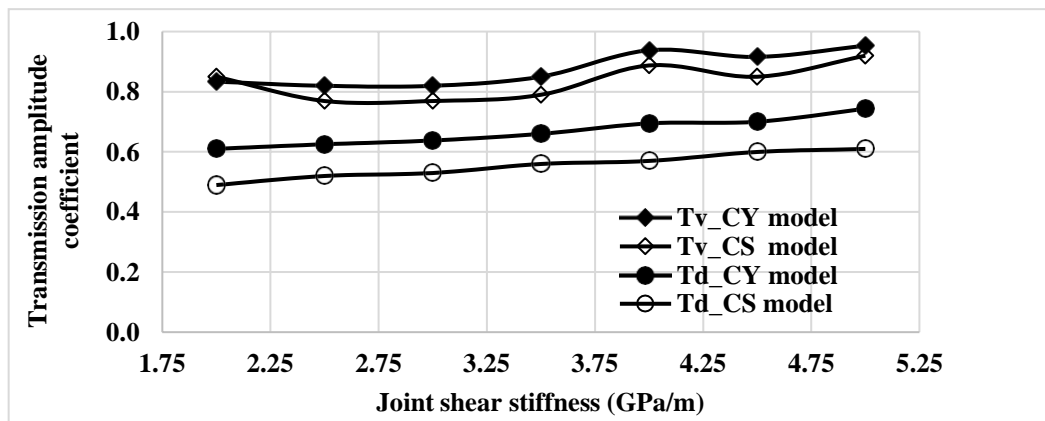


Fig. 8. (a) Transmission amplitude coefficients for different joint shear stiffness.

Joint normal stiffness (jkn)

For both CS and CY joint model, joint normal stiffness (jkn) value of 25 GPa/m was found out to validate numerical model. jkn was varied from 20 GPa/m to 30 GPa/m during numerical simulation without altering all other joint parameters. T_v and T_d did not show significant changes with change in jkn. T_v and T_d values for CY joint model were found to be higher than the CS joint model.

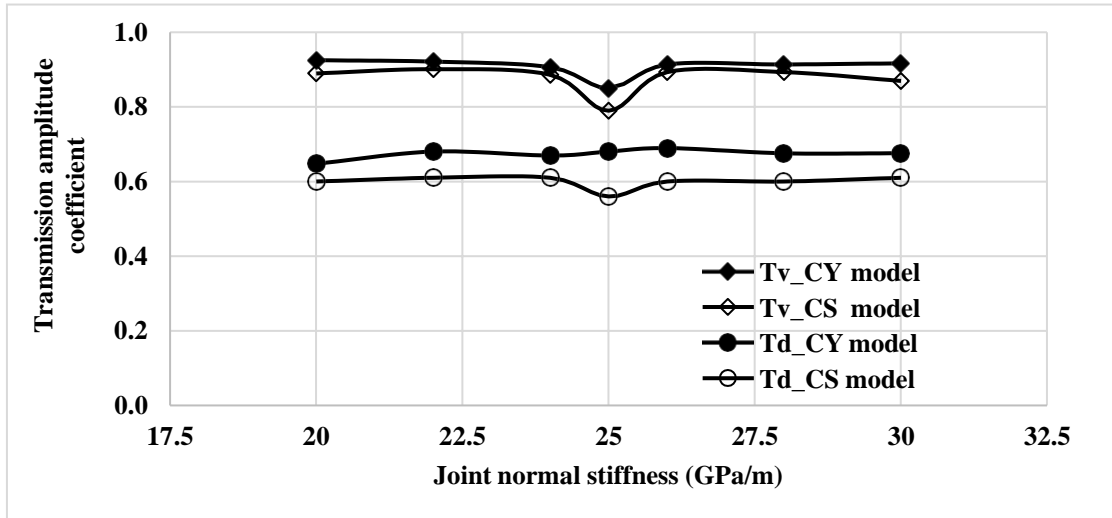


Fig. 8. (b) Transmission amplitude coefficients for different joint normal stiffness

Joint cohesion (jcoh)

Validated joint cohesion value for both the CS and CY joint model was found out to be 5 MPa/m. It was varied in range of 3.5 GPa/m and 6.5 GPa/m during numerical simulation, while all value of all other joint parameters were kept same. T_v and T_d did not vary much with change in jcoh. Transmission amplitude coefficients values for CS model were found to be lesser than the values obtained from CY joint model.

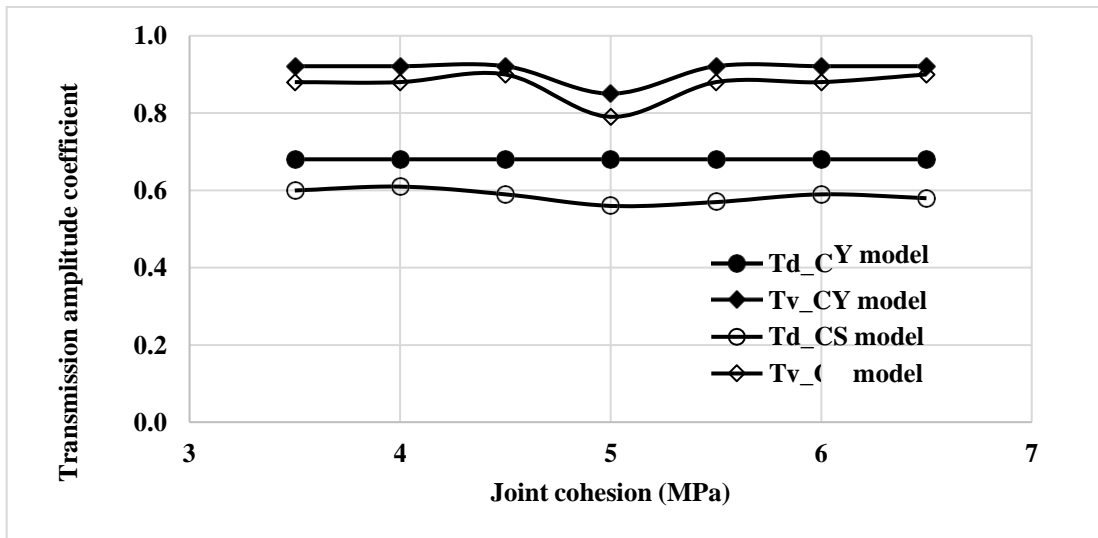


Fig. 8. (c) Transmission amplitude coefficients for different joint cohesion

Joint friction angle (jfric)

The joint friction angle (jfric) of 25° has been found out to validate the numerical model for both CS and CY joint models. Jfric was varied from 17.5° to 32.5° during numerical simulation without altering the value of all other joint parameters. T_v and T_d did not vary with change in jfric. T_v and T_d values for CY joint model were found to be higher than for the CS joint model.

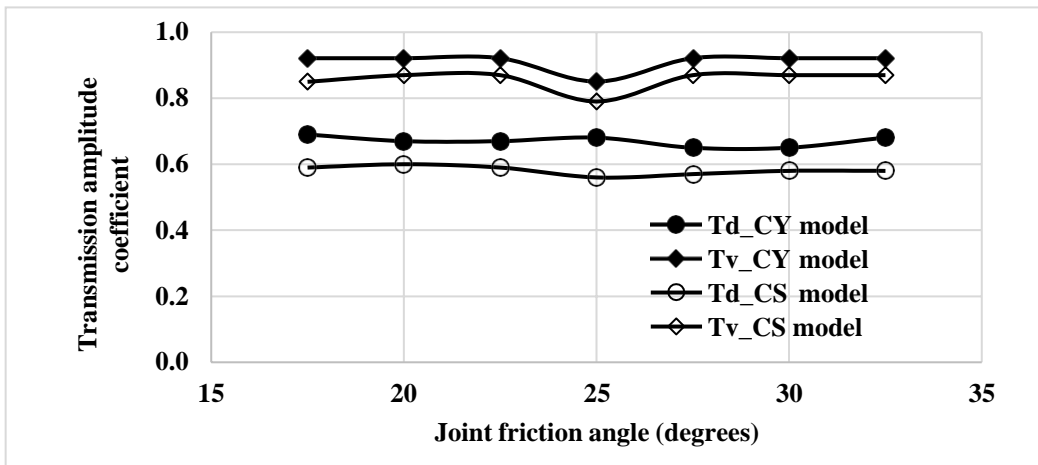


Fig. 8. (d) Transmission amplitude coefficients for different joint friction angles

Normal stress (insitu stress)

The value of normal stress provided between start and end of granite plates used for the validation of the numerical model was 0.5 MPa. It was varied from 0.35 MPa to 0.70 MPa during numerical simulation keeping values of all other parameters constant. T_v and T_d were found to be unchanged with change in insitu stress. Transmission amplitude coefficients values for CS joint model were found to be lower than that of the CY joint model.

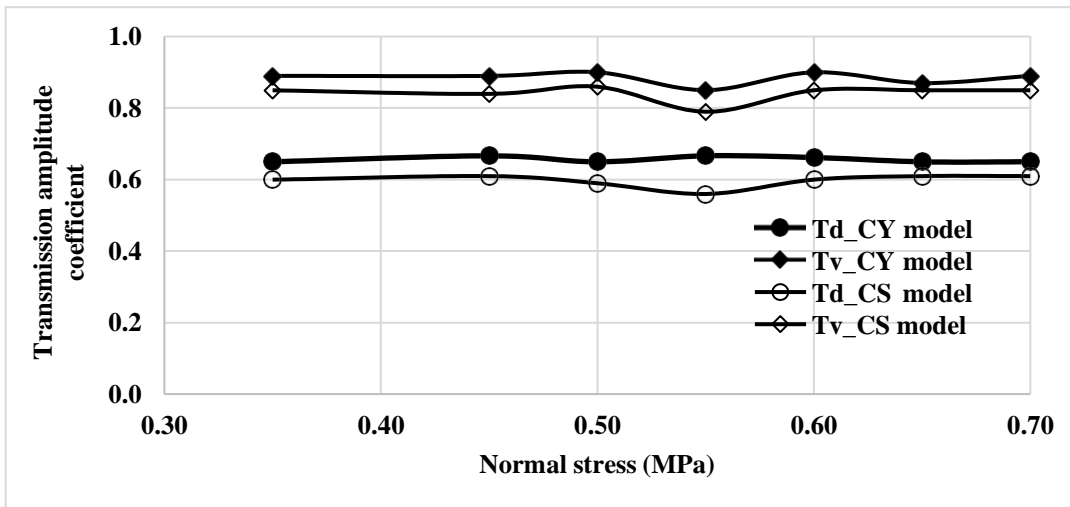


Fig. 8. (e) Transmission amplitude coefficients for different normal stress

Velocity coefficient (yvel)

Velocity coefficient (yvel) is defined by ratio of recorded real particle velocity and the particle velocity provided to the numerical model. For example, if recorded actual particle velocity is 1000 mm/sec, providing a yvel value as 0.005 means the 3DEC code will provide velocity of 5 mm/sec to the simulated model. Validated velocity coefficient value for both the CS and CY joint models was found out to be (-)0.0050. It was varied from (-)0.0035 to (-)0.0065 during numerical simulation without varying other joint parameters. T_v and T_d were found to be unchanged with change in yvel. T_v and T_d values for CY model were found to be higher than in the CS joint model.

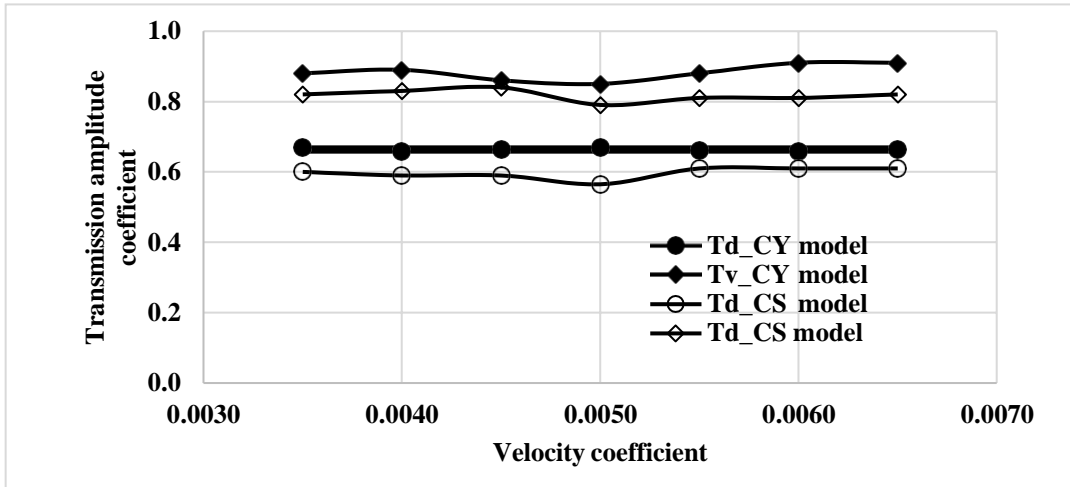


Fig. 8. (f) Transmission amplitude coefficients for different velocity coefficient

Table 5. Comparison of T_v and T_d values obtained from parametric studies

Parameters	Unit	Range				
		CY joint model		CS joint model		
		T_v	T_d	T_v	T_d	
Joint shear stiffness	GPa/m	2.00-5.00	0.83-0.95	0.62-0.75	0.76-0.91	0.48-0.61
Joint normal stiffness	GPa/m	20-30	0.86-0.92	0.65-0.69	0.79-0.90	0.56-0.61
Joint friction angle	Degrees	17.5-32.5	0.86-0.92	0.64-0.72	0.79-0.86	0.57-0.60
Normal stress	MPa	0.35-0.65	0.88-0.92	0.64-0.66	0.78-0.85	0.57-0.61
Joint cohesion	GPa/m	3.50 to 6.50	0.85-0.90	0.65-0.67	0.79-0.85	0.56-0.61
Velocity coefficient		(-)0.0035- (-)0.0065	0.85-0.91	0.66-0.67	0.79-0.84	0.57-0.61

Both the CS and CY joint model shows a similar trend for T_v and T_d for any joint parameter. For the CS joint model, both Transmission amplitude coefficients are lesser than that of the CY model.

5 Conclusions

The experiments on the SSP setup were conducted to determine the energy coefficient and transmission amplitude coefficient in terms of particle velocity and particle displacement (T_v and T_d). Energy coefficients were determined using peak particle velocities obtained from the experimental tests. Numerical simulation of the SSP setup was done to compare both the parameters mentioned above. For CY joint model, there is less difference between peak particle velocity before and after the joint. This observation holds true for particle displacement also. It indicates progressive damage of the joint material, as the wave continues to propagate through rock mass across the joint. For CS joint model, there is noticeable difference between peak particle velocity and displacement before and after the joint.

The following conclusions are drawn from the present study.

- 3DEC can be successfully used for simulating the wave propagation in jointed rock mass.
- Both the CS and CY joint model shows similar trend for T_v and T_d for any joint parameter. For the CS joint model, both T_v and T_d is lesser than the CS model.
- Joint shear stiffness is a valuable parameter that determines the transmission of shear wave across rock joints.

- Joint normal stiffness, joint friction, joint cohesion, velocity coefficient and normal stress do not have much influence on the shear wave transmission, for the values used in the numerical simulation.

6 Acknowledgments

This research is supported by Science and Engineering Research Board (SERB), Department of Science and Technology (DST), India, through the research project, No: ECR/2018/001966.

References

1. Jaramillo, C. A. (2017). Impact of seismic design on tunnels in rock – Case histories, *Underground Space*, 2(2), 106-114. <https://doi.org/10.1016/j.undsp.2017.03.004>
2. Lin, C. C. J., & Chai, J. F. (2008). Reconnaissance report on the China Wenchuan earthquake May 12, 2008. *NCREE Newsletter*, 3(3), 1-5.
3. Shimizu, M., Saito, T., Suzuki, S., Asakura, T. (2007). Results of survey regarding damages of railroad tunnels caused by the Mid Niigata Prefecture Earthquake in 2004. *TunnUndergr*, 38(4), 265- 273.
4. Yashiro K, Kojima Y (2007) Historical earthquake damage to tunnels in Japan and case studies of railway tunnels in the 2004 Niigataken-Chuetsu Earthquake. *Quarterly Report of RTRI* 48(3):136–141 DOI: 10.2219/rtriqr.48.136
5. Auld, B.: Cross-hole and down-hole vs by mechanical impulse. *Journal of Geotechnical Engineering Division, American Society Civil Engineers* 103, GT 12 (1977), pp.1381–1398.
6. McCann, D.M. and Baria, R.: Inter-borehole seismic measurements and their application in rock mass assessment. In: *Geophysical Investigations in Connection with Geological Disposal of Radioactive Waste, Proceedings of a Nuclear Energy Agency OECD Workshop*, Ottawa, 1982, pp.123–135.
7. King, M.S., Myer, L.R. and Rezowalli, J.J.: Experimental studies of elastic-wave propagation in a columnar-jointed rock mass. *Geophysical Prospecting* 34(8) (1986), pp.1185–1199.
8. Pyrak-Nolte, L.J., Myer, L.R. and Cook, N.G.W.: Anisotropy in seismic velocities and amplitudes from multiple parallel joints. *Journal of Geophysical Research* 95(B7) (1990a), pp.11,345–11,358.
9. Pyrak-Nolte, L.J., Myer, L.R. and Cook, N.G.W.: Transmission of seismic waves across single natural joints. *Journal of Geophysical Research* 95(B6) (1990b), pp.8617–8638
10. Myer, L.R., Pyrak-Nolte, L.J. and Cook, N.G.W.: Effects of single joint on seismic wave propagation. In: *Proceedings of ISRM Symposium on Rock Joints*, Loen, 1990, pp.467–473.
11. Zhao, J., Zhao, X.B. and Cai, J.G.: A further study of P-wave attenuation across parallel fractures with linear deformational behavior. *International Journal of Rock Mechanics and Mining Sciences* 43(5) (2006a), pp.776–788.
12. Li, J.C. and Ma, G.W. Experimental study of stress wave propagation across a filled rock joint, *Int J Rock Mech Min Sci* 46(3) (2009), pp. 471–478.
13. Dowding, C.H.: Estimating earthquake damage from explosion testing of full-scale tunnels. *Adv. Tunnel Technology and Subsurface Use* 4(3) (1984), pp 113–117.
14. Dowding, C.H.: *Blasting Vibration Monitoring and Control*. Prentice-Hall, NJ, USA, 1985.
15. Dowding C.H.: *Construction Vibrations*. New Jersey, Prentice-Hall, 1996.
16. Clough, R.W.: The finite element method in plane stress analysis. *Proceedings of the Second ASCE Conference on Electronic Computation*, Pittsburg, PA, 1960.
17. Malvern, L.E.: Introduction. In: *Mechanics of a Continuous Medium*. Englewood Cliffs, New Jersey: Prentice Hall, 1969
18. Shi, G.H.: Discontinuous Deformation Analysis, A New Numerical Model for the Statics and Dynamics of Block Systems. *PhD thesis*, Univ. of California, Berkeley, Berkeley, Calif, 1988.
19. Cundall P.A.: A computer model for simulating progressive large-scale movements in blocky rock systems. *Proceedings of the Symposium of ISRM*, Nancy, France, 1971, Vol.1, pp.11–18.
20. Liu, T., Li, J., Li, H., Li, X., Zheng, Y., & Liu, H. (2017). Experimental Study of S-wave Propagation Through a Filled Rock Joint. *Rock Mechanics and Rock Engineering*, 50(10), 2645-2657. DOI: 10.1007/s00603-017-1250-y
21. Wu W, Zhao J (2014) A dynamic-induced direct-shear model for dynamic triggering of frictional slip on simulated granular gouges. *Exp Mech* 54:605–613. doi:10.1007/s11340-013-9823-5
22. Miller, R. K. (1977). An approximate method of analysis of the transmission of elastic waves through a frictional boundary. *Journal of Applied Mechanics*, 44, 652-656. DOI:10.1016/0148-9062(79)90465-0

23. Miller, R.K. (1978). The effects of boundary friction on the propagation of elastic waves. *Bulletin of the Seismological Society of America*, 68(4), 987 – 998. DOI:10.1016/0148-9062(79)90465-0
24. X. F. Deng, J. B. Zhu, S. G. Chen., and J. Zhao . “Some Fundamental Issues and Verification of 3DEC in Modeling Wave Propagation in Jointed Rock Masses” *Rock Mech Rock Engineering* DOI 10.1007/s00603-012-0287-1
25. Kuhlemeyer, R.L. and Lysmer, J. “Finite element method accuracy for wave propagation problems.” *Journal of Soil Mechanics and Foundation Division, ASCE* 1973; 99 (5): 421-427.
26. Cundall, P. A., and R. D. Hart. “Analysis of Block Test No. 1 Inelastic Rock Mass Behavior: Phase 2 — A Characterization of Joint Behavior (Final Report),” Itasca Consulting Group Report, Rockwell Hanford Operations, Subcontract SA-957, 1984.
27. Cundall, P. A., and J. V. Lemos. “Numerical Simulation of Fault Instabilities with a Continuously Yielding Joint Model,” in *Rockbursts and Seismicity in Mines*, pp. 147-152. C. Fairhurst, ed. Rotterdam: A. A. Balkema, 1990.